

See discussions, stats, and author profiles for this publication at: <https://www.researchgate.net/publication/305776528>

# Serially Connected Monolayer MoS<sub>2</sub> FETs with Channel Patterned by a 7.5 nm Resolution Directed Self- Assembly Lithography

Conference Paper · June 2016

DOI: 10.1109/VLSIT.2016.7573376

CITATIONS

0

READS

45

10 authors, including:



**Amirhasan Nourbakhsh**

Massachusetts Institute of Technology

34 PUBLICATIONS 356 CITATIONS

SEE PROFILE



**Amir Tavakkoli**

Massachusetts Institute of Technology

16 PUBLICATIONS 256 CITATIONS

SEE PROFILE



**Jing Kong**

Massachusetts Institute of Technology

300 PUBLICATIONS 17,564 CITATIONS

SEE PROFILE



**Karl K. Berggren**

Massachusetts Institute of Technology

261 PUBLICATIONS 6,508 CITATIONS

SEE PROFILE

Some of the authors of this publication are also working on these related projects:



Scaling and transport properties of two-dimensional materials transistor [View project](#)



superconducting nanowire single-photon detectors [View project](#)

All content following this page was uploaded by [Ahmad Zubair](#) on 02 April 2017.

# Serially-Connected Monolayer MoS<sub>2</sub> FETs with Channel Patterned by a 7.5 nm Resolution Directed Self-Assembly Lithography

A.Nourbakhsh, A. Zubair, A. Tavakkoli, R. Sajjad, X. Ling, M. Dresselhaus, J. Kong, K. K. Berggren, D. Antoniadis and T. Palacios  
Massachusetts Institute of Technology, Cambridge MA 02139, USA, Email: anour@mit.edu

**Abstract:** We demonstrate sub-10 nm transistor channel lengths by directed self-assembly patterning of monolayer MoS<sub>2</sub> in a periodic chain of homojunction semiconducting-(2H) and metallic-phase (1T') MoS<sub>2</sub> regions with half-pitch of 7.5 nm. The MoS<sub>2</sub> composite transistor possesses an off-state current of 100 pA/μm and an  $I_{on}/I_{off}$  ratio in excess of  $10^5$ . Modeling of the resulting current-voltage characteristics reveals that the 2H/1T' MoS<sub>2</sub> homojunction has a resistance of 75 Ω.μm while the 2H-MoS<sub>2</sub> exhibits low-field mobility of ~8 cm<sup>2</sup>/V.s and carrier injection velocity of ~10<sup>6</sup> cm/s.

**Introduction:** 2D crystals of layered transition metal dichalcogenides (2D-TMDCs) such as MoS<sub>2</sub> are ideal candidates for aggressive miniaturization of field-effect transistors (FETs) to the single digit nanometer scale. In addition to large bandgap, chemical stability and compatibility with CMOS processes [1, 2], this class of materials can benefit from their atomically thin body with dangling-bond-free surfaces. Because of this and their ultra-small body thickness which leads to very small electrostatic characteristic scaling length,  $\lambda = \sqrt{(\epsilon_s \cdot t_s \cdot t_{ox} / \epsilon_{ox})}$ , transistor subthreshold swing (SS) and drain-induced barrier lowering (DIBL) coefficient in such films can be significantly smaller than for conventional thin-body semiconductors. In particular, monolayer-MoS<sub>2</sub> (ML-MoS<sub>2</sub>), because of its bandgap of 1.8 eV yields high  $I_{on}/I_{off}$  ratio MOSFETs, while its low dielectric constant,  $\epsilon_s = 4-7$ , and atomically thin body,  $t_s \approx 0.7$  nm, facilitate the reduction of  $\lambda$ . In our previous work [3], we reported a 15-nm channel length MoS<sub>2</sub> FET using monolayer graphene as the Source/Drain (S/D) contacts. In this work, by exploiting the semiconducting to metallic phase transition in MoS<sub>2</sub> [4], we demonstrate a sub-10-nm transistor channel length by patterning of MoS<sub>2</sub> in a periodic chain of homojunction semiconducting- (2H) and metallic-phase (1T') MoS<sub>2</sub> regions. The 2H- to 1T'-phase transition occurs by exposing 2H-MoS<sub>2</sub> to *n*-butyl lithium solution as confirmed by electrical and photoluminescence measurements (Fig.1). Sub-10 nm 1T'/2H MoS<sub>2</sub> patterning is achieved by directed self-assembly (DSA) of block copolymers (BCP) technique which is one of the most promising emerging technologies for cost-effective, nanoscale, and high-volume manufacturing [5].

**Device Fabrication:** The key steps for fabricating BCP patterned MoS<sub>2</sub> FETs, as well as a schematic of the devices are shown in Figs. 2 and 3, respectively. ML-MoS<sub>2</sub>, grown by chemical vapor deposition (CVD), was transferred onto a [p<sup>+</sup> Si/native SiO<sub>2</sub>] substrate coated with 10 nm of HfO<sub>2</sub> (EOT ≈ 4 nm) serving as the back gate (BG). Subsequently, by means of electron beam lithography and Au metallization, end-contacts to the MoS<sub>2</sub> film and measurement pads were formed. Next the surface of the substrate is functionalized with hydroxyl terminated polystyrene (OH-PS), poly(styrene-*b*-dimethylsiloxane) (PS-*b*-PDMS) BCP solution is spun-on followed by a solvent vapor annealing step to promote microphase separation, and finally selective reactive ion etching (RIE) of PS matrix is done in a controlled O<sub>2</sub> plasma leaving behind oxidized-PDMS (ox-PDMS) lines parallel to the Au lines. Fig.4a shows the final ox-PDMS lines with half-

pitch of 7.5 nm formed between Au lines contacting the MoS<sub>2</sub> film. Next, the phase transition treatment of the ox-PDMS-patterned MoS<sub>2</sub> is applied to selectively convert the uncovered underlying 2H-MoS<sub>2</sub> to 1T'-MoS<sub>2</sub>, while the ox-PDMS-covered regions remain semiconducting. These alternating 2H-MoS<sub>2</sub>/1T'-MoS<sub>2</sub> areas correspond to semiconducting and metallic regions with same length, and form a chain of transistors in series as shown in Fig. 4b. The resulting transistor pitch is equal to the BCP period, 15 nm, with channel length of 7.5 nm. The minimum number of transistors-in-series thus formed between a pair of 120-nm-spaced Au electrodes was 8.

**Results and discussion:** Fig. 5a shows the  $I_d$ - $V_g$  evolution at three fabrication stages of an eventual chain of eight ML-MoS<sub>2</sub> FETs with 15 nm pitch. As can be seen, the ML-MoS<sub>2</sub> survives the PS etching step and still shows high  $I_{on}/I_{off}$  modulation. However, current degradation of more than two orders of magnitude is observed as well as higher SS and shifted threshold voltage ( $V_t$ ) compared with the as-fabricated MoS<sub>2</sub>-FET. These changes are the consequences of the MoS<sub>2</sub> surface being affected by the plasma radicals. The unwanted degradation is nevertheless direct indication that the PS film is fully etched and the gaps between PDMS lines are fully opened. The last  $I_d$ - $V_g$  curve in Fig. 5a shows the same device characteristics after phase-transition treatment. Fig 5b shows the final device at different  $V_d$  values highlighting the significant increase of  $I_{off}$  at  $V_d=1$  V, which can be attributed to direct source-drain tunneling in the individual FETs. Fig. 6a shows the model fit to the data using the MIT Virtual Source model [6]. The transfer curve below threshold is determined by the MoS<sub>2</sub> threshold voltage (~ -1V), gate capacitance (for 4 nm EOT) and carrier velocity (8x10<sup>5</sup> cm/s). Near and above threshold ( $V_g > 0$  V), the contact resistance (~20 kΩ.μm) dominates over the channel resistance until the Schottky contact resistance between the Au metal and MoS<sub>2</sub> is sufficiently low (~1 kΩ.μm for  $V_g > 2$  V). In this regime ( $V_g > 2$ V), the channel resistance dominates again and the transport is determined by carrier mobility ( $\mu \approx 8$  cm<sup>2</sup>/V.s) and series resistance between 1T'/2H MoS<sub>2</sub> homojunction (~ 75 Ω.μm). Fig. 6b shows the predicted transfer characteristics of an idealized single 7.5 nm MoS<sub>2</sub> transistor assuming MoS<sub>2</sub>-metal contact resistance of 100 Ω.μm, and double gate with appropriate work-function and EOT of 0.5 nm leading to a drastically improved SS (62 mV/dec), low DIBL (~20 mV/V) and higher ON current. The carrier velocity and mobility found here from the modeling of the experimental devices are comparable to previously estimated values [7-9]. With the current CVD growth technique, the  $I_{on}$  is 0.1 mA/μm for  $I_{off} \approx 10$  pA/μm at  $V_d=0.5$  V (Fig. 6b). Further improvement of carrier velocity is possible with improved film-growth method to meet ITRS requirements for future nodes. **Conclusions:** We have demonstrated the operation of MoS<sub>2</sub> FETs with the shortest and thinnest S/D channel, namely ~7.5 nm long and ~0.7 nm thick, reported to date. The transistor chain shows  $I_{on}/I_{off} \approx 10^6$  with  $I_{off} \approx 100$  pA/μm. Further improvement of  $I_{on}$  current is possible by improved growth of MoS<sub>2</sub> and thus increased carrier velocity and mobility to meet the current requirement for high performance.

**Acknowledgments:** Partial support by the ONR PECASE program and the NSF NEEDS program.

**References:**

- [1] B. Radisavljevic, *et al.*, Nat. Nano. Vol. 6, no. 3, p 147, 2011
- [2] W. Cao *et al.*, IEDM 2014.
- [3] A. Nourbakhsh *et al.*, VLSI 2015.
- [4] R. Kappera *et al.*, Nat. Mat. Vol. 13, p 1128, 2014
- [5] S. Jeong *et al.* Mater Today 16, 468-476, 2013.
- [6] A. Khakifirooz *et al.*, IEEE T Electron Dev. 56, 1674, 2009.
- [7] W. Cao *et al.*, IEEE T Electron Dev. 2014.
- [8] M. Luisier *et al.*, IEDM 2014.
- [9] G. Fiori *et al.*, APL 2013

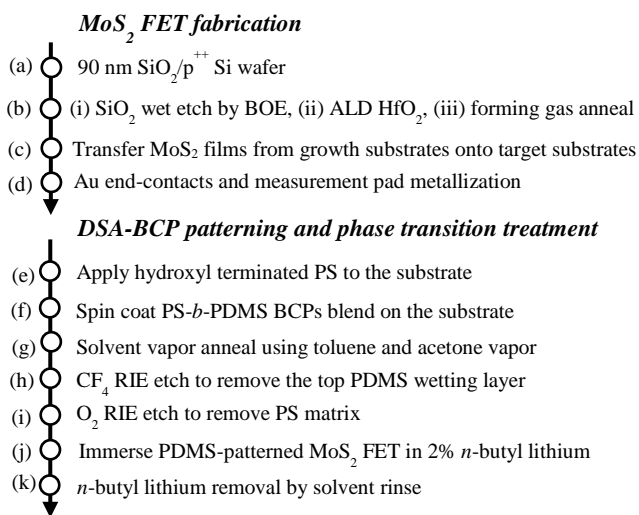


**Fig. 2.** Fabrication process flow of the short channel 1T'/2H MoS<sub>2</sub> FETs patterned by DSA-BCP technique. Step (b) includes ALD-HfO<sub>2</sub> at 200 °C, followed by annealing in a forming gas at 400 °C.

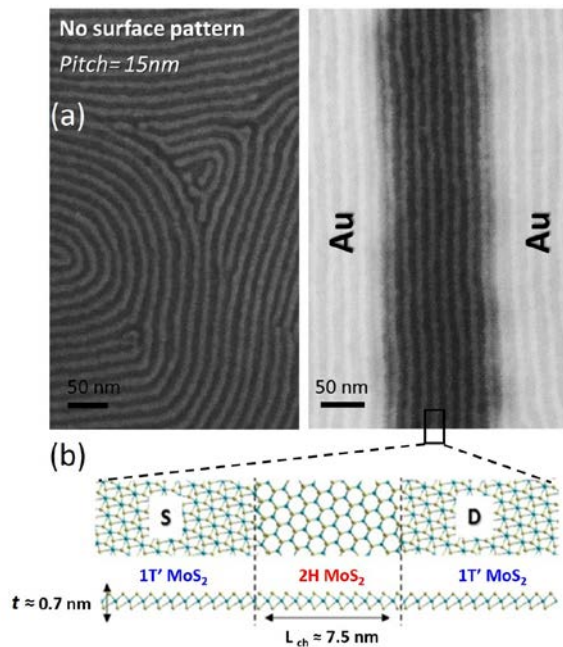


**Fig. 4.** (a) SEM images show ox-PDMS lines with 15 nm pitch after PS etch on surfaces with no guide pattern as well as surfaces with Au lines as directional guides. The absence of pattern leads to random formations of the ox-PDMS lines while in patterned surface lines are self-assembled in parallel with the Au electrodes. (b) Schematic short channel FET comprised of a 2H-MoS<sub>2</sub> channel contacted to two adjacent metallic 1T'-MoS<sub>2</sub> regions forming S/D contacts.

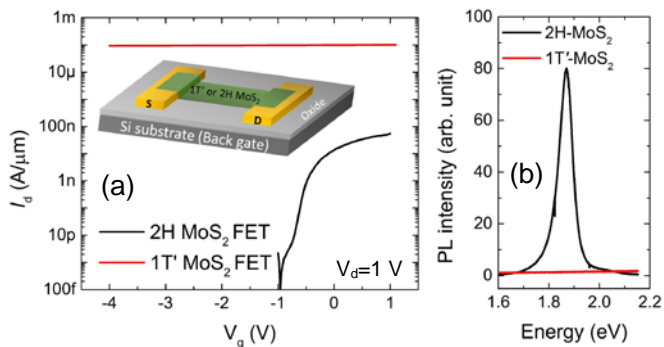


**Fig. 1.** (a)  $I_d$ - $V_g$  of a long-channel MoS<sub>2</sub> FET before and after phase transition treatment. The intrinsic 2H-MoS<sub>2</sub> FET shows strong semiconducting behavior with large gate modulation, while after the phase transition, it shows constant (compliance) current due to metallic 1T'-MoS<sub>2</sub>. (b) PL spectra of monolayer 2H- and 1T'-MoS<sub>2</sub>: The 2H phase shows a strong PL peak at 1.85 eV, while the PL of the 1T'-phase is absolutely quenched owing to its gapless metallic characteristics.

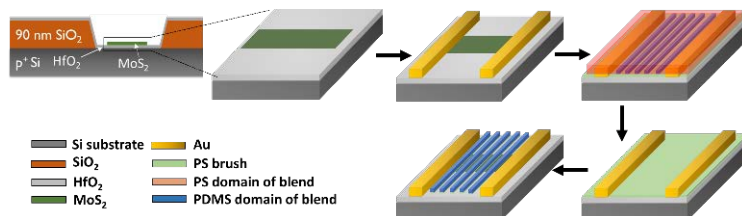


**Fig. 3.** Schematics depicting the different steps of the DSA of BCP on MoS<sub>2</sub> FETs

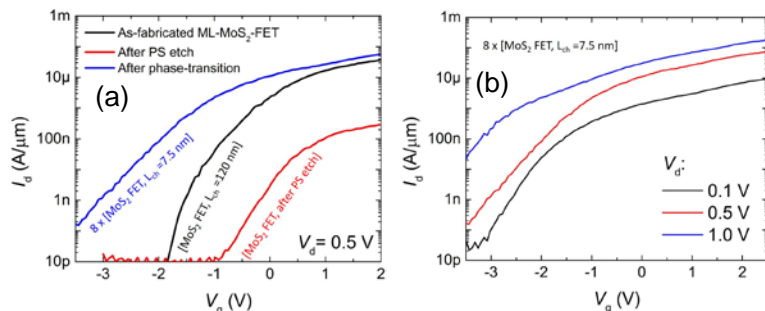


**Fig. 5.** (a) Evolutions of  $I_d$ - $V_g$  at  $V_d = 0.5$  V of a CVD monolayer MoS<sub>2</sub>-FET: As-fabricated (black), after PS etch (red) and final (blue) after phase transition treatment with *n*-butyl lithium. (b)  $I_d$ - $V_g$  of the final device (8x MoS<sub>2</sub> FETs,  $L_{ch}=7.5$  nm) at different  $V_d$  values.

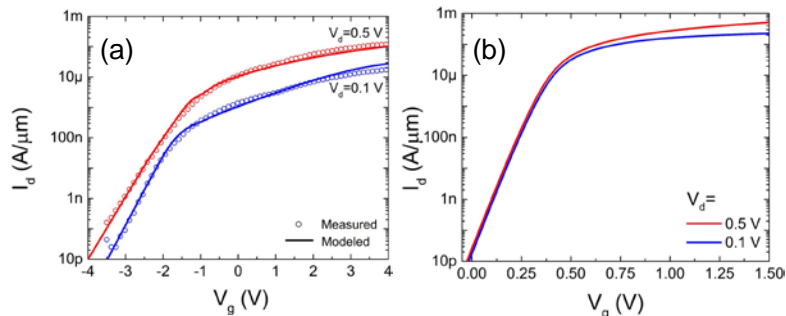


**Fig. 6.** (a) MVS fit of the experimental data for the 8 transistor array, high end-contact resistance dominates transport above threshold and limits the  $I_{on}$  below 100  $\mu$ A/ $\mu$ m. (b) Performance prediction of a single transistor with a double-gate structure, EOT of 0.5 nm, and with the same device parameters but assuming excellent contact resistance (100  $\Omega$ . $\mu$ m). Threshold voltage is adjusted to +0.5V for this plot.